Journal Pre-proofs

Catalytic Microwave Preheated Co-pyrolysis of lignocellulosic biomasses: A study on biofuel production and its characterization

P. Jennita Jacqueline, V. Shenbaga Muthuraman, C. Karthick, Abed Alaswad, G. Velvizhi, K. Nanthagopal

PII: S0960-8524(21)01724-7
DOI: https://doi.org/10.1016/j.biortech.2021.126382
Reference: BITE 126382

To appear in: *Bioresource Technology*

Received Date: 7 October 2021
Revised Date: 15 November 2021
Accepted Date: 16 November 2021

Please cite this article as: Jennita Jacqueline, P., Shenbaga Muthuraman, V., Karthick, C., Alaswad, A., Velvizhi, G., Nanthagopal, K., Catalytic Microwave Preheated Co-pyrolysis of lignocellulosic biomasses: A study on biofuel production and its characterization, *Bioresource Technology* (2021), doi: https://doi.org/10.1016/j.biortech.2021.126382

Catalytic Microwave Preheated Co-pyrolysis of lignocellulosic biomasses: A study on biofuel production and its characterization

P Jennita Jacqueline [a], V Shenbaga Muthuraman[b], C Karthick [b], Abed Alaswad[c], G Velvizhi[d], K Nanthagopal [b*]

[a] School of Chemical Engineering, Vellore Institute of Technology, Vellore-632014, India

[b]Engine Testing Laboratory, School of Mechanical Engineering, Vellore Institute of Technology, Vellore-632014, India

[c] School of Engineering and Applied Science, Aston University, UK.

[d] Centre of CO_2 research, Vellore Institute of Technology, Vellore-632014, India

* Corresponding author email address: nanthagopal2013@gmail.com

* Corresponding author Contact number: +91 9943928066

Abstract

In this present study, microwave pre-treatment has been used for sustainable biofuel production from three different biowastes through catalytic aided co-pyrolysis techniques. The experimental investigations have been carried out to develop biofuel at temperature (350-550℃), heating rate (15-50℃/min) and particle size (0.12-0.38mm). The resultant biofuels were characterized using TGA, DTA, FE-SEM, FTIR spectroscopy and NMR spectrum. The pyrolysis process of biomasses without and with catalyst resulted in the yield rate of 29-37% and 39-51% respectively. Moreover, the CaO catalytic co-pyrolysis process of pomegranate peel, groundnut shell and palmcone wastes with a ratio of 50:50 at 0.25mm particle size has resulted in the highest yield rate of 51.6%. The NMR result of bio-oil samples produced hydroxyl group and aliphatics which clearly state the suitability of bio-oils for automotive application. The bio-oil had promising fuel characteristics consisting more energy density (29.1MJ/kg), less oxygen content and free of nitrogen.

Keywords: Pyrolysis; Lignocellulosic Biomass; Bio-oil; CaO catalyst; Renewable fuel

1. Introduction

Sustainable alternative energy plays a significant role in environmental changes. In the past few decades, industrialization and population growth rate is intimated by the energy demands (Suriapparao et al., 2020). The majority of energy demand is highly contributed to fossil fuels like coal, natural gas and petroleum resources. However, the consistency in these fossil fuel utilization results in not only environmental problems but also causing sustainability issues. Therefore, global energy demand is compensated by several renewable energy resources (Varma et al., 2019). In reason times, biomass is getting a wider attraction for sustainable energy development due to the enormous route of raw materials. It does not only used to produce heat but also for chemical products, electricity generation and more importantly fuels which can compensate for global energy to some extent. Many developing countries have developed numerous effective waste management systems and for the disposal of various biomass resources however complete disposal causes a financial crisis, and polluting the environment and in particular filling up the occupying landfill sites (Arenas et al., 2019). The applied waste management strategy for biofuel production has been presented in Fig.1. The word biomass refers to organic plants, trees, agricultural industrial residues also including municipal solid waste which is all sun's energy of photosynthesis. Even today the biomass contributes 12% of the primary energy supply in the world and many developing countries to the range of 40-50% (Demirbaş and Arin, 2002). Waste recycling will have creative eco-social business models that are the more cascading and circular economy. Furthermore, the waste valorization process requires a development of an efficient and sustainable waste management strategy to overcome the limitations of conventional waste management approaches.

Bio-oil is the promising alternative fuel in the current scenario, promoting renewable energy resources and is made up of lignocellulosic biomass via the pyrolysis process (Wu et al., 2020) Biomass is the third-largest renewable energy source in the world's energy supply (Zhang et al., 2021). Biomass and waste can be converted through thermochemical conversion processes such as pyrolysis, gasification and combustion (Arenas et al., 2019). Pyrolysis is gaining popularity because it can produce a variety of value-added products in the form of gases, liquids, or solids, depending on the process conditions (Neves et al., 2011). Biomass from lignocellulosic sources (LCB) is one of the most promising options for reducing fossil energy dependency, as it is the only renewable source that contains carbon that can produce biofuels similar to fossil fuels (Karthick & Nanthagopal., 2021). Moreover,

the major portion of biomass derived from plants, woods, and crops is lignocellulosic in the form of hemicellulose, cellulose and lignin. The use of lignocellulosic biomass like organic-based biomasses as a potential feedstock for biofuels, energy, and biorefinery applications is focussed among the scientific community (Ferreiro et al., 2017). Pyrolysis of biomass in the absence of oxygen at high temperatures (450–600 °C) is referred to as biomass pyrolysis. Depending on the operating conditions and reactor category, this technology has the potential to produce a liquid fraction (bio-oil) yield of 60–70 wt.% (Singh et al., 2020). Pyrolysis is divided into two types based on heating rates: fast pyrolysis and slow pyrolysis. The consumption of biomass for biofuels and biorefinery production is being complex method due to the involvement of several key factors including the utilization target, conversion expenses, accessible technologies, storage and distribution (Sakulkit et al., 2020). There have been numerous biomass resources for the production of bio-oil and biochar like corn cobs, coconut shells (Rout et al., 2016), wheat straw (Suriapparao et al., 2020), coffee grains (Matrapazi and Zabaniotou, 2020), fruit peels (mango, banana, pomegranate, orange, etc.) (Arenas et al., 2019), rice straw and rice husks (Hao et al., 2021), rubberwood, oil palm biomass (Sakulkit et al., 2020) and wood sawdust (Soni and Karmee, 2020).

The advanced technology of co-pyrolysis is one of the emerging and promising approaches for the effective recovery of biomass for various resources. Bio-oil obtained through the pyrolysis process is seems to be highly oxygenated which has resulted in low heating value, enhanced acidity, significant humidity content. All these issues lead to poor storage stability (Vuppaladadiyam et al., 2021). An effective way of mixing two or more biomass feedstocks is commonly known as the co-pyrolysis technique which has shown much improvement in the end products without much energy consumption. Moreover, the higher yield rate co-pyrolysis technique is highly influenced by individual components of biomass (Volpe et al., 2018). Sourabh Chakraborty et al. (Chakraborty et al., 2021) examined the co-pyrolysis process using digested sludge, algal biomass and cedarwood for the production of bio-oil through thermochemical techniques. Even though the co-pyrolysis technique has reduced the oxygen content in the resultant products, the bio-oil extracted rate is slightly higher than other conventional pyrolysis (Zhao et al., 2020). This low yield rate could be enhanced with the presence of a suitable catalyst. Several catalysts have been developed so for the improvement of higher production of bio-oil around the globe. The function of catalyst the co-pyrolysis technique is to crack the highly volatile compounds into simplified form deoxygenation, dehydration and decarboxylation techniques (Ren et al.,

2020). In recent times numerous catalysts have been used like biochar-based zeolite catalysts, Fe-based catalysts, metal oxides catalysts (CaO, TiO_2 etc.) Ni-based catalysts and more importantly microporous composites catalysts (Hao et al., 2021). Metal oxides have gained focus in catalytic pyrolysis processes, due to their convenience and accessibility. It was also found that metal oxides were efficient for oxygen elimination (Lin et al., 2018). CaO converted the glycosidic bond breakage route to the breakdown and reforming route, as seen by the lowering of levoglucosan and acetic acid. CaO also aided the side-chain detachment reaction mechanism in lignin, leading to an increase in phenol and diols (Veses et al., 2014). CaO, a classic basic oxide, has been investigated as a catalyst for bio-oil improvement due to its environmental compatibility and low cost. Through catalytic processes, CaO aided in the production of hydrocarbons. Furthermore, CaO removed the acids while increasing the selectivity of the ketones. Meanwhile, when compared to non-catalytic pyrolysis, the amounts of hydrocarbons and light chemicals (such as acetaldehyde and acetone) were considerably enhanced (Lu et al., 2010).

In recent years, pyrolysis process is one of the best biofuel development methods for the conversion of waste biomass into wealthy biofuel energy. In addition, highly integrated pyrolysis with suitable pre-treatment like ultrasonic, hydrothermal carbonization, microwave and pickling could enhance the bio-oil extraction rate at an economically viable route. Among which microwave pre-treatment is the predominant method that has resulted in a higher yield rate on biomass conversion. Hardly a few experimental works only carried out with microwave preheated pyrolysis process. Specifically, the unique selection of various biomass mixtures from different waste sources for the co-pyrolysis is a novel work. However, there is no research outcome on the influence of metal oxide on bio-oil production. Therefore, an attempt has been made to investigate the impact of Calcium oxide (CaO) on bio-oil production from various biomass feedstocks. A comparative assessment has been carried out on bio-oil production from with and without catalyst activation under the same operating conditions. Further, this study has been extended to enhance the bio-oil production rate using the co-pyrolysis approach and evaluation of bio-oil for the suitability in internal combustion engines.

2. Materials and Methods

2.1. Biomasses preparations

The present investigation was carried out on various lignocellulose biomasses of pomegranate peel (PP), groundnut shell (GS) and palm cone waste (PCW). These biomasses have better volatile compounds of higher than 75% and more than 45% of hemicellulose content. These biomasses are collected from different waste sources like groundnut shell from agro waste, pomegranate peel from food waste and palm cone from the forestry waste. Primarily the collected biomasses were cleaned using deionized water and dried in the presence of sunlight for 48 hrs duration. Thereafter, the size of biomasses was grinding to the particle size of 0.12-0.38mm for achieving a better yield rate. These biomasses were heated up to 65℃ in a hot air oven for 24hrs duration to drain out the moisture content. The ultimate analysis of biomasses used in the present investigation is given below. In the end, biomasses samples were kept inside the desiccator to avoid moisture absorption. The biomasses and products characterization all the pyrolysis experiments and instruments analysis given in Table 1.

2.2. Microwave pre-heated treatment

In this study, biomass samples were undergone a microwave pre-treatment process using a microwave oven. These samples were heated at the rate of 545.95, 818.91 and 887.16W/min for 3min, 3min and 2min respectively. The optimized pre-treatment condition was tabulated in Table 2 and catalyst proportions are provided in Table 3. After completion of the pre-treatment process, the weight of the biomass samples is estimated and recorded for further investigation. the entire production process of formulated in the form of a flow chart which is given in Fig.2.

2.3. Pyrolysis Experimental Setup

The present experimental work was conducted on a pyrolysis reactor of 2litres capacity. It consists of two condensation units, an inbuilt electrical furnace, a chiller unit, and a vacuum pump. The internal diameter of the quartz reactor is 100mm and the height is 320mm which can withstand the temperature upto 1500^0c. A 2kW external furnace has been installed in the system for the heating purpose and the reactor temperature controlled by an external PID controller. The vapour obtained from the reactor is directed to the condensation unit for the condensation process. Finally, the bio-oil was collected from the round-bottom flask and the weight of bio-oil was measured. In addition, the weight of biochar is also measured and the yield percentage of the pyrolysis products is calculated using the below-mentioned equations

(1-3). In the end, the reactor was cooled to ambient temperature after the completion of the pyrolysis process and the biochar left in the reactor was collected.

$$\text{Bio oil yield\%} = \frac{\text{weight of the collected biooil}}{\text{weight of the biomass}} \times 100 \quad (1)$$

$$\text{Biochar yield\%} = \frac{\text{weight of the collected biochar}}{\text{weight of the biomass}} \times 100 \quad (2)$$

$$\text{Gas yield\%} = 100 - (\text{Bio - oil yield \%} + \text{Biochar yield \%}) \quad (3)$$

The production of bio-oil from various biomass feedstocks was investigated in two production methods like non-catalytic and catalytic co-pyrolysis process. Initially, the dried microwave preheated samples of pomegranate peel (PP), Groundnut shell (GS) and Palm cone waste (PCW) were explored non-catalytic pyrolysis process. Each biomass sample was taken as 150g with a particle size of 0.12-0.38mm were placed in the reactor, and all the samples were heated at the rate of 15-50℃/min to find the final heating temperature for maximum biomass conversion. In the second phase of the investigation, co-pyrolysis was used by mixing these biomasses at a 50:50 ratio without catalyst. In the third stage, the co-pyrolysis process was enhanced by a CaO catalyst for the same biomasses blend under the same operating conditions.

2.4. CaO catalyst

From the extensive technical literature, the metal oxide can boost up the pyrolysis reaction under any specified operating condition. Numerous metal oxides are existing and many oxides were used successfully for bio-oil production. A comparative study on various metal oxides for the upgradation of the pyrolysis process was studied with ZnO, Cao, MgO, TiO_2, NiO and Fe_2O_3. Among these metal oxides, ZnO has the ability to slightly alter the pyrolysis product and Fe_2O_3 has the potential to form the hydrocarbons. But none of these metal oxides except CaO has the potential to eliminate the acids and formation of hydrocarbons (Lu et al., 2010). So that, in this present study calcium oxide (CaO) was used as a catalyst for co-pyrolysis reaction due to its better cracking ability to split the carbon chain into smaller molecules without deriving the higher temperature. In an earlier study wang et al, suggested that foundation materials such as inexpensive dolomite and limestone could be more advantageous in improving pyrolysis oil output (Wang et al., 2010). It was also pointed out that utilization of CaO for co-pyrolysis reaction does not produce carboxylic acids or furans because these carboxylic acid present would greatly reduce the bio-oil production. At the same time, the CaO catalyst could enhance the yield of Ketones, phenols, alkenes, and

alkadienes (Lin et al., 2018). For all the catalyst co-pyrolysis reactions, the catalyst was crushed and sieved to a 200-mesh size before usage, and the powders were dried at 120°C for 2 hours to eliminate the physically absorbed water.

2.5. Water content titration

Karl Fischer's water analysis is currently carried out using two separate methods: volumetric and coulometric titration. A sample water content determines the method. Iodine solution is added to each tube using a motorized piston burette in the volumetric Karl-Fischer titration. The volumetric titration is appropriate for samples with a high water content, ranging from 0.01 to 100% by weight. Iodine is produced in the coulometric Karl-Fischer titration by electrochemical oxidation in the titration cell. This approach is appropriate for samples with low/trace water content ranging from 0.0001 to 5% by weight. On the titrator, the water content of each tested sample (standard and oils) was determined in the same way. The sample weighed between 0.10 and 0.15g. When the drying oven reached the desired temperature, the sample was dropped into it with a dropper. The DM 143 SC electrode was utilized for the titration, and the "mixing time" was set to 60 seconds (the start of the measurement – insertion of the sample into the sample tube), the titration itself was 900 seconds, and the "delay time" was set to 60 seconds (60 seconds from reaching the first endpoint to the moment the titration ended). The Karl-Fischer technique was used to measure the amount of residual water in the organic phase (Zhen et al., 2020).

3. Results and discussion

3.1. Biomass Characterization

3.1.1. Ultimate analysis of Raw materials and biochar

The ultimate analysis could determine the fuel's properties in the specified substrate and the results are summarized in Table 4. The elemental analysis showed that the contents of C, H, N, S and O of PP, GS, PCW were in the range of 40-55%, 5-6.7%, 0.5-1%, >0.01% and 40-50% respectively. Similarly, the biochar products have the C, H, N, S and O in the range of 75-80%, 3-5%, 0.1-0.5%, 0.01 and 15-18% approximately. In both raw biomasses and biochar, the amount of carbon and oxygen is higher than hydrogen, nitrogen, and sulphur, according to the ultimate analysis. The C and H levels of PP were greater than among GS and PCW, whereas the N, S, and O levels of PP were lower than among GS and PCW. The oxygen concentration of biomass must be low for the pyrolysis process, while the carbon and hydrogen levels should be high. This is because the carbon and hydrogen in biomass can be

transformed into valuable aromatic chemicals in bio-oil (Sakulkit et al., 2020). On the other side, during the pyrolysis process, oxygen will be coupled with the hydrocarbon molecules as oxygenated compounds, lowering the quality of bio-oil. Furthermore, pyrolysis of biomass with a high oxygen concentration poses a risk of producing bio-oil with high water content. This is due to the formation of moisture content by the chemical reaction between hydrogen and oxygen (Pimenidou and Dupont, 2012). The nitrogen and sulphur levels of the biomass samples were also low. It was also noted that the formation SOx and NOx were extremely low in all biomass samples due to their low inherent rate. The biochar retains the majority of sulphur and nitrogen (Varma et al., 2019). From the available elemental analyzer data, the empirical formula for the raw biomasses and biochar were obtained and the same has been presented in Table 4. Further, the H/C and O/C molar ratio was calculated by the empirical formula. Finally, the higher heating value (HHV) was also estimated from the elemental composition biomasses using the Dulong equation (Table 4) (Park et al., 2011)

3.1.2. TGA and DTA analysis

Thermogravimetric analysis (TGA) and Differential thermal analysis (DTA) are determining the nature of thermal stability of biomass characterization. The thermal behaviour of PP, GS, and PCW was carried out in a non-reactive environment using a TGA and DTA instrument (SDT Q600). Around 2.25mg sample was taken for each biomass sample to characterize the thermal stability in the range of 30-800℃. The heating was carried out at the rate of 20 ℃/min with a constant flow of N_2 gas purge 100ml/min. The thermal breakdown of PP, GS and PCW was presented in Fig.3. Decomposition happened mostly during the drying phase, active pyrolysis phase, and lastly char production stage, according to the TGA and DTA Curve representation of biomasses. For the drying, active pyrolytic phase, and passive pyrolytic stage, the thermal decomposition temperatures of biomass ranged from 30-150°C, 150-550°C, and 550-800°C respectively (Mishra et al., 2019). The peak of the TGA curve was majority shown in between 120-600℃ is represented as temperature range biomass in the pyrolysis process active phase. The DTA curve identifies the majority of components decomposed in the range of 400-600℃ which makes it suitable for the pyrolytic condition (Mishra and Mohanty, 2020). The TG curves of the three biomasses (PP, GS, and PCW) were compared, and PCW and GS were in the more or less same temperature range as PP. A similar trend has been noticed in the DTA curve also. The PP biomass is manifested thermal stability beyond the expected temperature but in the experimental method of co-pyrolysis, PP biomass has not shown any influence on yield rate. Higher molecular weight compounds,

such as heavy hemicellulose and cellulose compounds, were partitioned into lower molecular fractions by external thermal effects in the second stage at the pyrolytic phase of 120-600°C resulted in the liberate of hot volatiles. Because of the degradation of hemicellulose in the first phase (120-350°C) and cellulose in the second phase (350-550°C), the second phase is divided into lower and intermediate temperature ranges. However, this temperature range may vary depending on the content of the biomass. In comparison to cellulose and lignin, hemicellulose is less thermally stable. Nevertheless, at high temperatures (> 550 °C), the hydroxyl phenolic groups that improved lignin's thermal resilience will be discussed in FTIR analysis. There was no further weight loss in the passive zone, but carbon and ash were present in solid form (inorganic residue). It was also noted that the final heating temperature of all pyrolytic experiments was maintained at 550℃(Mishra and Mohanty, 2020).

The samples of 2.24 mg for PP, 1.434 mg for GS and 2.174 mg for PCW were taken in the TGA and DTA analysis experiments. From Fig.3(a), it is identified that PP, GS, and PCW biomasses were dried in the range of 6.043%, 6.870%, and 8.558% in the 0.136mg, 0.099mg, and 0.186mg, respectively. The biomass samples consumed in the active pyrolytic stage as 1.192 mg, 0.732 mg, and 1.029 mg at rates of 53.03%, 50.44%, and 47.33% for PP, GS, and PCW, respectively. The results verified that higher molecules degraded into lower compounds as hemicellulose decomposed in cellulose to achieve the greatest peak shown in the DTA curve. The final TGA curve clear indication of char formation which can be directly correlated by the presence of lignin content in the biomass samples. Interestingly all three biomass samples were produced biochar residue at beyond 500℃. The char residue in PP, GS, and PCW biomasses are 8.816% in 0.1982mg, 7.678% in 0.111mg, and 12.52% in 0.277mg, respectively. The residual component of the TGA analysis revealed that a large number of biomasses were either entirely converted to char or degraded. The pyrolytic conditions have completely devoured that stage of the sample, leaving just residual biomass. The values are 32.11% in 0.722mg for PP, 30.05% in 0.503mg for GS and 31.58% in 0.687mg for PCW biomasses respectively.

In the DTA curve (Fig.3(b)) these three peaks are thought to be caused by various lignin, hemicellulose, and cellulose breakdown ranges, according to the literature. The initial curve of DTA analysis inveterate that water molecules and lower molecular weight compounds were removed in the earlier stage and the values are 0.069℃ min/mg and 0.0101℃ min/mg at 62.88℃ and 298.59℃ for PP biomass, 0.0744℃ min/mg at 64.96℃ for GS biomass and 0.139℃ min/mg at 63.34℃ for PCW biomass respectively. PP biomass has enlarged

molecular weight compounds with biomass closer to the apex of hemicellulose. This result is verified by the DTA curves in which a desorption phenomenon is linked to an endothermic peak. The DTA curves below 90°C have shown a likely weight loss due to water desorption remaining in samples. Moreover, hemicellulose decomposition has been verified at peaks detected at 89.78° C, 83.94° C and 81.65° C for PP, GS and PCW biomasses as hemicellulose degraded typically at a lower temperature of 80 °C to 340°C. The maximum temperature for the co-pyrolytic reaction is limited to 550℃ due to subsequent cracking reactions beyond 600°C which enhances the gas formation and also diminishes bio-oil production. Some of the earlier studies stated that effective pyrolysis conversion could be possible even at a temperature of 450-500℃ which is very low compared to the present investigation. However, in this study 550℃ is seems to be the best temperature for pyrolysis conversion which has been proved from the curves of DTA. Fig.3(b) revealed that the weight loss of biomass samples was quite low at higher temperatures and this trend has been witnessed in all the biomass samples during the pyrolysis technique. The thermal degradation of biomass samples begins beyond 250℃. The cellulose breakdown has effectively happened at two locations 320.85℃ and 583.5℃ for PP biomass whereas for GS biomass at 561.9℃ and PCW biomass 559.4℃. The DTA analysis has evident that PP biomass has more potential to yield bio-oil even at extreme temperature levels.

3.1.3. FTIR Characterization

Fourier Transform Infrared Spectroscopy analysis was conducted using an FTIR analyzer (MODEL: Thermo Nicolet iS50 with inbuilt ATR made by Thermo Fisher Scientific). The FTIR characterization analysis was carried out at different stages of biomass samples, which confirms the occurrence of diverse functions in connection with different chemical classifications. It was evident that the functional substances and functional groups along with the characteristic absorption bands for all biomass samples which are prepared under co-pyrolysis technique with and without catalyst. The peak value of the FTIR spectrum at the range 3500-4000cm^{-1} was a representation of water content which is due to the stretching vibration of OH radicals for the presence of alcohols, phenols and water particles in the biomass samples (Zhang et al., 2021). It is also witnessed that the same peak value for water content was derived as 3641.60cm^{-1} for all the co-pyrolysis biomass samples. On other hand, the same peak value was obtained from the biochar sample as well. Furthermore, the presence of lignin content in the biomass samples was evident at 3229.42cm^{-1} and 3294.42cm^{-1}. These bands can be attributed to OH stretching vibrations associated with cellulosic compounds

(Zhang et al., 2020). The remaining CH radicals are induced by symmetrical and asymmetrical stretching of CH_2 which has been found in 2922.16cm^{-1} (Liu et al., 2016). The higher peak value of 1700-1650cm^{-1} in the FTIR spectrum was the clear indication of C=O based ketones and this has resulted in the conversion of aldehyde to ketones by the breakdown of hemicellulose and cellulose compounds (Zhang et al., 2020). In the present FTIR analysis, the ketones were noted at the peak of 1718.58 cm^{-1} and 1724.36 cm^{-1}. The OH bending mode of adsorption water and protein amide C=O is primarily responsible for the wideband at 1620.2cm^{-1} (Liu et al., 2016). The aromatic C=C stretching vibration was identified at 1614.42cm^{-1}, and the pattern in these four samples are nearly identical (Hu et al., 2021). The existence of monocyclic, polycyclic, and substituted aromatic compounds is shown by the absorption band of 1410-1650cm^{-1}. The FTIR spectrum of the biochar sample shows the peak value of 1411.89cm^{-1} which is the presence of C-H stretching of aromatics in the lignin structure, however the same has been revealed at 1423cm^{-1} and 1424cm^{-1} in co-pyrolysis biomass samples (Lazzari et al., 2018).

On the other hand, the non-esterified carbonyl group has been traced out at a peak of 1328.95cm^{-1} in the co-pyrolysis biomass samples. These peak ranges provide strong C-H stretching during the catalyst-based co-pyrolysis reaction. The peak spanning 1200-1100cm^{-1} can often be due to organic acid C-O stretching (Yang et al., 2007). The existence of phenols and alcohols generated by the breakdown of hemicellulose, cellulose, and lignin was suggested by the -OH and C-O stretching associations at the peak value of 1228.66cm^{-1} and 1147.65cm^{-1} respectively (Yang et al., 2007). Furthermore, the peak at 1228.66cm^{-1} in the MW FTIR spectra is due to the vibration mode of OH/NH deformation in proteins (Liu et al., 2016). The absorption peak at 1014.58cm^{-1} indicates the bending of C-O and C-O-H in secondary and primary alcohols or aliphatic ethers, however, catalyst assisted co-pyrolysis of biomass sample at the peak value of 1026.13cm^{-1} could reflect the vibrational stretching of C-O-H, C=C, C-C-O from polysaccharides (Ceylan and Goldfarb, 2015). These peak values were generated with strong intensity and high attribution during association with cellulose and hemicellulose of catalyst co-pyrolysis. The lower bandwidth 800-400cm^{-1} is a clear indication of CO_2 content (Zhang et al., 2020), however, in the present study peak value of 875cm^{-1} was noted in the biochar sample which is due to aromatic structure (Hu et al., 2021). The enhancement in the higher peak value is mainly due to the presence of a catalyst in the pyrolysis reaction. The remaining small traced amounts in the spectrum show the accumulation of different species.

3.2. Product yields

Pyrolysis studies were carried out to analyze the effect of various operating parameters on the final production rate. It is also used to conduct the in-depth properties estimation of bio-oil which is obtained from various forms of biomasses. Fig.4(a-c) shows the production of pyrolysis oil and other by-products through pyrolysis and co-pyrolysis techniques. It is well known that the pyrolysis oil yield rate is highly dominant by factors of heating temperature, heating rate, biomass particle size and more importantly feedstock compositions. Therefore, the entire experimental investigation was conducted at the peak temperature of 550°C. In particular, the heating temperature selection co-pyrolysis technique was selected based on the TGA data. It has been observed that the production of pyrolysis oil was maintained at 30-33% during individual pyrolysis techniques and it was enhanced to 36% during the non-catalytic co-pyrolysis technique. This result has been evident for all the co-pyrolysis biomass samples at the ratio of 50:50 (Hao et al., 2021). Further improvement in the production yield of pyrolysis oil was noticed during the catalytic-based co-pyrolysis technique. In particular, the highest yield rate of 51.7% was obtained for a co-pyrolysis combination of PP+ GS+ PCW+ CaO. The resulting liquid fraction is a complex combination of hydrocarbons ranging from C_5 to C_{20}, with a low heating value, a C/H ratio similar to that of many fuels, and a low sulphur level (Berrueco et al., 2005). From the graph, it is also interesting to note that the biochar production was slightly higher for PCW biomass during individual pyrolysis techniques and this biochar rate marginally reduced (40-44%) during the non-catalytic co-pyrolysis process. On the other hand, the CaO catalyst aided co-pyrolysis process has shown a remarkable reduction in biochar production and this reduction has been witnessed for all combinations of biomass samples.

The resultant residue of the pyrolysis technique was obtained from various biomasses in the form of residue loss and water content. The residual loss is explained as the segment of the glass column linking the upright condenser and bent at a 30° where tar or pyrolysis oil deposition occurred. The maximum pyrolysis oil deposited in that region was scraped off with a customized spatula. Following the pyrolysis process, the glass column, condensers, spatula, and vents connecting the condensers were thoroughly cleaned with acetone to reduce the loss caused by pyrolysis oil sticking to the glass equipment (Bhattacharjee and Biswas, 2019). The liquid fraction is the combination of oil and water content, the water content determined by the Karl-Fischer titration (Zhen et al., 2020), almost considered as a loss. Interestingly, the residue loss and water content are quite consistent (10-15%) during the

individual pyrolysis and non-catalytic co-pyrolysis process. However, the resultant residues were reduced substantially to below 10% during the catalyst-based co-pyrolysis process and this trend has been maintained for all combinations of biomass samples. This reveals that the presence of CaO catalyst is playing a more dominant role than co-pyrolysis biomass samples. It is generally known that in the case of co-pyrolysis, the presence of a catalyst caused a dehydration reaction, resulting in the creation of water, acid, and carbonyl compounds. In addition, the production of gases and char should be enhanced. Further, the addition of a catalyst in the raw materials can significantly improve the production of gases and pyrolysis oils (Fekhar et al., 2020). The pyrolysis process was carried out until no vapours emerged from the reactor as a result of employing the catalyst aided batch reactor. As a result, the formulation of heavy oil during the pyrolysis process was completely eradicated. In comparison among all catalytic processes is the highest yield of liquid fraction was obtained 45-51% during the catalyst co-pyrolysis process. In the present study, the CaO has been used as a cracking catalyst under a 50:50 catalytic co-pyrolysis ratio. This has resulted in $CaCO_3$ formation during the pyrolysis reaction which has enhanced the CO_2 capturing ability from these biomasses. Finally, it was concluded that the presence of CaO during the co-pyrolysis technique has shown remarkable improvement on resultant products and it is expected to increase with a higher concentration of CaO. Metal oxides catalyst CaO enhances the oil yield which makes up to lower gas yields, it is better suitable for lignocellulosic biomasses materials. To improve the effectiveness of the hemicellulose to cellulose decomposition catalyst CaO, the catalyst cracks the cellulose with the help of oxidation to increase the bio-oil upgrade. It's possible that using a CaO catalyst to promote cracking events will result in the synthesis of condensable organic compounds via retrogressive reactions, enhancing the liquid fraction yield. After the segregation of bio-oil from the yielded products in NMR analysis was carried out to identify the physical nature of sustainable bio-oil. Fig.4(d) depicts the overall resultant products obtained from catalytic and non-catalytic biomasses in percentage. Nearly 10-15% pyrolysis gas also formed during all pyrolysis methods which has a common issue in pyrolysis techniques.

The gas temperature differs between catalytic and non-catalytic runs. When CaO is used, an increase in H_2 concentration is noticed, as well as a slight increase in both CH4 and CO intensities and a decrease in CO_2. It could be owing to CO_2 capture by calcium-based components according to Equation (4), favors H_2 creation from the water gas shift reaction and, as a result, methane reforming according to Equation (5) and (6). It's important to note

that only CaO is taken into account in the carbonation reaction, which corresponds to the reduced concentration of CO_2 found in the CaO study.

$$CaO_{(s)} + CO_{2(g)} \leftrightarrow CaCO_{3(s)} \quad (4)$$

$$CH_{4(g)} + H_2O_{(g)} \leftrightarrow 3H_{2(g)} + CO_{(g)} \quad (5)$$

$$CO_{(g)} + H_2O_{(g)} \leftrightarrow CO_{(g)} + H_{2(g)} \quad (6)$$

$$\text{Biomasses} + CaO_{(s)} \xrightarrow{\Delta} \text{Syngas(g)} + \text{Biochar(s)} + CaCO_{3(S)} \quad (7)$$

$$\text{Syngas(g)} \xrightarrow[\text{condensation}]{} \text{Biooil(l)} + \text{tar(s)} \quad (8)$$

As these Calcium-based substances have shown a catalytic effect on biomass pyrolysis, the rising concentrations of H_2, CH_4, and CO could be attributed to improving cracking reactions as shown in Equation (7) and (8). As a result, for those studies with calcium-based materials, a higher HHV is obtained, with CaO containing this improved performance.

3.3. Influence of operating parameters on product yields

In this chapter, influential effect of various operating parameters involved in the pyrolysis process such as heating rate and particle size and catalytic loading has been discussed. Moreover, temperature of pyrolysis reactor has major role in influencing the bio-oil yield rate. But the optimum temperature has been chosen as 550^0C based on the TGA and DTA analysis results.

3.3.1. Effect of Heating rate

Thermal breakdown of PP, GS, and PCW biomasses was executed in the pyrolysis reactor under an inert atmosphere at multiple heating rates. The pyrolysis oil yield rate of PP, GS, and PCW biomasses at different heating rates experiment and three kinds of biomass are made up of non-catalytic and catalytic were co-pyrolyzed at 550℃ at different heating rates (15-50℃/min). The resultant products of non-catalytic and catalytic techniques are compared through oil yield rate only. The higher heating rate means that the biomass is exposed to higher temperatures for a shorter period, resulting in instability. The TG and DTA curves migrated nearer to the high-temperature area as the heating rate increased, and also thermal hysteresis has emerged in the pyrolysis process. In addition, as the heating rate was raised, the initial release temperature of volatile components and the peak temperatures of the DTA curves have increased. As the temperature range increased, the pyrolysis process reached its peak pyrolysis temperature before reaching its final pyrolysis temperature, at which bio-oil

was created and hemicellulose degradation to cellulose has occurred. With a rise in heating rate, the lower volatile matter deposition, low weight loss and higher residual weight were found and this trend was noticed with an increase in pyrolysis temperature also (see supplementary material). As pointed out earlier the TGA analysis clearly shows the three stages of the pyrolysis process which include the drying stage, heating stage and final stage. It is to be suggested from the DTA curve that the removal of moisture content and weight loss in the biomass samples would happen in the first phase of pyrolysis when the temperature reaches beyond 100℃. The pre-heating stage (100℃ ~ T_0; T_0 is the initial pyrolysis temperature) happens when the biomass depolymerizes and the "glass transition" starts. The volatiles is emitted in the third stage (T_0~T; T is the final pyrolysis temperature) (Xiao et al., 2020).

As the heating rate increases, the pyrolysis temperature reaches its maximum value, which makes the greater influence of pyrolysis oil yield rate. The cellulose decomposition along with lignin formation for the production of bio-oil is highly triggered during the second stage of the pyrolysis process (active pyrolysis phase). As per the given data, the raising final heating rate and the final pyrolysis temperature are proportional to a peak pyrolysis temperature. At the same time, increasing the heating rate might affect the oil yield rate. The inherent heat and mass transfer among biomass particles affect the pyrolysis characteristic temperature at different rates. At a lower heating rate, there is a uniform heat distribution among each biomass particle without much weight loss and this might result in enhancement pyrolysis production rate. Even though, when the heating rate rises, the temperature gradient between the interior and exterior surfaces of the biomass particles would be widened. Moreover, due to the lag in heat transfer rate, the pyrolysis temperature inside the biomass particles is very low. It affects the pyrolysis of the inside biomass particles. As a result, the pyrolysis of biomass happens at a wider temperature range by shifting the DTA peak towards higher temperature which makes a greater influence on lignocellulosic biomass particles development (Xiao et al., 2020). It was identified that with an escalation in heating rates from 15 to 50℃/min at a uniform rise of 5^0C/min in the active zone (about 150- 550℃), decomposition of non-catalytic co-pyrolysis (PP, GS and PCW) was observed 20%, 24.1%, 24.5%, 27.1%, 28.3%, 36.4%, 33.1%, 33% and catalytic co-pyrolysis (PP, GS, PCW with CaO) was 23%, 31%, 33%, 41.5%, 45.23%, 51.7%, 48.1% and 46% yield rate respectively as shown in Fig.5(a) and 5(b). At a heating rate of 40℃/min, both non-catalytic and catalytic co-pyrolysis are shown maximum oil yield and beyond 40℃/min heating rate, the yield rate

was slow down. The heating rate was estimated from using TGA results through optimized temperature limits. The reduction in the residence time at higher heating rates results in a slowdown in the interaction between the biomass particles. It also produces more inorganic residues at a higher heating rate. While maintaining prolonged residence time, the interaction between biomass particles has decreased the inorganic residue formation even at lower heating rates (Mishra and Mohanty, 2020).

3.3.2. Effects of Particle Size distribution

The particle size distribution on different biomass at a heating rate of 40°C/min was influenced. In the case of Groundnut shell and palm cone waste biomasses, the initial and final pyrolysis temperature enlarged for large particles but were comparable for small particles (0.12-0.18mm and 0.22-0.38mm) at the same heating temperature. However, for Pomegranate peel (PP) biomass the particle size distribution was revised as it seems to be the heftiest. This is due to the woody structure of both GS and PCW biomasses in nature and this has resulted in larger interparticle spaces. Interestingly, the lower thermal resistance between the interior surface of smaller biomass particle sizes offered better pyrolysis efficacy with a superior yield rate. On the other hand, the higher particle size of biomass samples produced a lower yield rate. It is to be noted that an increase in biomass particle sizes (0.12-0.38mm) required a higher initial temperature of 213- 267°C and this trend has been witnessed in non-catalytic and catalytic co-pyrolysis (See supplementary material). Therefore, maintaining a smaller particle size for each biomass sample is the topmost priority to attain the initial temperature. In the present study, the PP biomass has been identified as higher intensity with smooth structure in the form of smaller particle size. However, as per the TGA result, the weight loss curves of GS and PCW biomasses occupies high-temperature area which has resulted in higher semi-char yield even though these particle sizes were low. On the other hand, this trend seems to be inverse in PP biomass with two intermediate temperatures and therefore the addition of PP with GS and PCW biomass samples could enhance the intermolecular reaction among biomass particles. This is primarily the heat-transfer constraint in and around the particles that generates a temperature difference inside the granules during the pyrolysis of large particles(Xiao et al., 2020). The heat transfer rate reduced as particle size surged, and the time is taken for heating the particle nucleus to rise to the final reaction temperature has been enhanced. The results revealed that the particle size (0.12-0.15, 0.18-0.22 and 0.25-0.38mm) on both non-catalytic co-pyrolysis were observed to be 33.65%, 33.4%, 35.2%, 36%, 36.4%, 35.4% and for catalytic co-pyrolysis was 42.4%, 43.6%,

45.56%, 45.21%, 51.7% and 46% yield rate respectively as shown in Fig.5(c) and 5(d). Moreover, the weight loss in biomass samples has been revealed during the microwave preheated process due to the changes in its surface area and also the removal of moisture content. The maximal weight loss, Umax (%/°C) has slightly increased with an increase in a final pyrolysis temperature and followed decreasing trend after the attainment of peak temperature. As a result, considering the cost and reaction control factors, 0.25mm was determined to be the optimum particle size for the three raw materials in this investigation. Even though, both non-catalytic and catalytic co-pyrolysis yielded a higher oil rate at a particle size of 0.25mm, catalyst-based co-pyrolysis resulted in higher output. This is due to the change in particle structure on microwave preheated biomass along with the presence of catalyst thereby producing a higher yield rate (Varma et al., 2019).

3.3.3. Effects of microwave preheating and catalyst loading on pyrolysis process

In this study, the microwave preheating has been performed to enhance the thermal cracking of biomass for obtaining better bio-oil yield. When comparing the pyrolysis processes of individual biomasses with and without microwave preheating process, the process with microwave preheating process has better yield rate. Because, the experimentation process without microwave preheating of individual biomasses results in 20-25% of bio-oil yield rate. On the other hand, the pyrolysis process of individual biomasses aided with microwave preheating shows the improved yield rate of 29-32%. Moreover, the co-pyrolysis of biomass mixtures results in further improved yield rate of 33-37%. Besides, both the individual biomasses and their mixtures achieved the optimum yield rate at the microwave oven setting condition of 545W/min for 3min. Additionally, the yield rate achieved for each biomass and their mixtures at various microwave preheating condition are presented in table 2 and the yield rate ranges are represented as higher (40-50%), average (30-40%), and lesser (20-30%). To determine the influence of microwave preheating using the FE-SEM analysis method, the morphological characteristics and surface microstructure of CaO with biomass samples were studied. FE-SEM images show that the microwave preheated biomasses produce variation in particle size distribution which has resulted in different surface structure (see supplementary material). The purpose of this study was to look at the physical effects of microwave preheated PP, GS, and PCW biomasses at various powers as listed in Table 2 and the effect of catalytic aided process as listed in Table 3. In general, the untreated biomass samples have complete block structures. Further, it also has flat and smooth surfaces with just a little quantity of debris on the entire particles. The surface structure of biomass could be destroyed

by microwave pretreatment, and the lignin layer from the interstices in the packed microfibrils framework could be removed (Kainthola et al., 2019). The effect of catalyst loading on individual biomass with CaO catalyst was investigated, and the bio-oil yield was found to be in the expected range of 39-44%. Each biomass yield has various strategies and produces a diverse fraction of bio-oil yield. Furthermore, the experiments were conducted in catalytic co-pyrolysis to achieve a higher yield. In the end, the addition of CaO catalyst on microwave preheated biomass samples yielded higher bio-oil and it also has an impact on active pores which has changed the structural-functional group. It can be seen that the lignocellulosic structure of the untreated biomass samples remains intact, there are no pores on the surface. While adding CaO catalyst with biomass sample, it was covered by the upper surface of the biomass. The heterogeneous sample of raw biomasses was shown in 3.4µm (approx.) and the catalyst surface pores of 36.25µm were depicted. As the CaO belongs to nanopores structure, its presents in the lignocellulosic biomass enhance the interaction among biomass particles with much impact of cohesive efforts (Liang et al., 2019). Further, the active pores of CaO could absorb the moisture content of biomass and it also accelerates the oxidation reaction. Due to these inherent changes, the pore sizes are reframed into microfibrils which leads to a crackdown of the lignocelluloses and thereby much improvement in the pyrolysis process. The microfibrils structure pores of 2.06µm (approx.) and the catalyst CaO completely blended with biomass samples i.e. the interior surface of biomass which react with CaO and the structure was smoothy surface of nanopores of 2.515µm (Zhang et al., 2021). EDS analysis noticed that the value of oxygen is less to compare the CHNS analysis which means CaO absorbs the water molecules helps to oxidation reaction. The percentage of EDS analysis mentions that Ca (54.2%), O (32.9%) and C (12.9%) respectively. The CaO is one of the best cracking catalysts which could modify the functional group of the biomasses through interaction between the inner and outer surface of biomasses. This reaction has cracked down the cellulose and upgraded the bio-oil via the condensation of gases.

The peak pyrolysis temperature (θmax) values of CO_2, CO, and CH_4 shift to lower temperatures in the CaO catalytic run, while the θmax values of hydrocarbons and other oxygenated compounds shift to higher temperatures (Wang et al., 2010). Due to its substantial basicity, CaO was the best co-pyrolysis deoxygenation catalyst. It has the highest alkene selectivity, which indicates that the bio-oil is of higher quality. However, due to coke production during the pyrolysis process, the CaO exhibited a considerably lower total peak

area for volatile chemicals than uncatalyzed pyrolysis (Lin et al., 2018). The biomasses with a higher quantity of co-pyrolysis improve the pyrolysis efficiency, as CaO catalyst absorbs and converts microwave into heat before dissipating them to the biomasses. Biomasses with a low CaO fraction, on the other side, have a lower potential for decomposition due to their poor heat transfer efficiency (Mong et al., 2020). Furthermore, the high fraction of CaO catalyst mixed with biomasses relatively exhibits a low conversion rate of 50%, as indicated by the high level of liquid yield (50% wt). This is owing to the role of CaO catalyst as microwave absorber which plays a pivotal role in the conduction heat exchange process within the biomasses. The microparticle size of 0.25mm for both the CaO catalyst and the biomasses enable superior surface contact for effective heat transfer thus allowing the biomass samples temperature to attain a higher level. Fig.6 (a) shows 50-60% proportion of CaO enhances the higher yield of bio-oil through microwave preheating catalytic co-pyrolysis technique.

3.4. Bio-oil Characterization

Nuclear Magnetic Spectroscopy is one of the finest techniques that have been popularly used for the estimation of the composition, molecular structure and purity of any solid/liquid matter. In this present study, NMR was used for analyzing the chemical structure of bio-oil which has been developed through pyrolysis and co-pyrolysis processes due to its faster response with a better signal to noise (S/N) ratio (Hao et al., 2016). All the bio-oil samples obtained from the investigation were dissolved in acetone (d_6) before being subjected to the NMR spectrum. The existence of ammonium formate signal in some samples suggests that not all H-donor molecules decayed under the circumstances used. This is especially relevant for samples with a high concentration of H-donor(Struhs et al., 2021). Since the pyrolysis process was used for bio-oil production the ^{1}H and ^{13}C NMR study has been deployed for the evaluation of H-C functional groups. It has been noticed that the resultant bio-oil yielded from various biomasses mainly consists of aliphatic and hydroxyl groups and lesser aromatic given in Table 5. In particular, ring-join methylene (Ar-CH_2-O)/ ether and a slight portion of an aliphatic structure of CHβ and CHγ are the unwanted products that need to be removed. Further, the presence of ring-join methylene is a clear indication of better anti-knocking behavior and is thereby suitable for automotive application. The majority of H-NMR peaks are seen between 0.5 and 3.0 ppm, which is associated with –CH_3 and –CHn–. (aliphatic region). This means that the bio-oil produced comprises mostly aliphatic components and only a trace of aromatic compounds (McIntosh et al., 2021). It is also evident that the CHγ

exists in the range of 1-1.9ppm, which is very minimum in all the bio-oil samples. Notably, the non-catalytic co-pyrolysis process showed higher CHγ output as 3.66%. in comparison with conventional petroleum products, CHγ ring compounds would enable better combustion during chemical reactions with oxygen. The bio-oil extracted through individual pyrolysis from PP biomass exhibited a higher hydrogen percentage of 136.84% and a similar same trend has been noticed in TGA analysis as well. All the NMR spectrum of bio-oils showed only a marginal quantity of β- CH3 (2.02-3.0ppm) which is considered as an impurity (See supplementary material).

In the absence of the ammonium formate signal, significant increases in the normalized intensity of signals for -aliphatic protons closed to heteroatoms or unsaturation are seen. The signals of the ether and methoxyl groups are likewise greatly influenced. These findings point to hydrogen incorporation into certain functional groups found in bio-oil molecules (Struhs et al., 2021). The pattern related to water in the pyrolysis oil sample is around 3 to 4 ppm. Interestingly, ring-join methylene (hydroxyl group) seems to be the peak in the range of 3.2-3.77ppm during the non-catalytic co-pyrolysis technique. Further, the hydrogen concentration was extremely high (174.47%) this formulation was reversed due to the addition of a CaO catalyst. However, due to the addition of CaO catalyst, this hydroxyl group seems to be extremely low and this is due to the presence of moisture content in the PP biomass sample. In this situation, the minimum level is preferred because, unlike the high concentration sample, the sharp peak at 3.3-3.7ppm is not overlapped on the water signal (2.9–3.7ppm) (Smets et al., 2011). The systematic removal of hydroxyl compounds from renewable bio-oil would enhance the possibilities of using them as automotive fuels. The in-depth NMR results also revealed that the biomass structure, size and inherent composition play a vital role in hydroxyl group formation. From the NMR results, the addition of during co-pyrolysis exhibits the minor value (0.29%) of impurities when compared to non-catalytic co-pyrolysis. Among all the tested biomass samples, the individual PP biomass and CaO based co-pyrolysis showed the phenolic group in the range of 5.1-5.29ppm which is clear evidence of OH radicals aromatic structure/ alkenes present in the bio-oils. These OH radicals would offer better anti-knocking behaviour during a chemical reaction. It is also concluded that CaO addition during co-pyrolysis produced more volatile compounds for all the biomass combinations. The key benefits of using NMR to analyse bio-oils are that (1) the entire bio-oil can be diluted in a suitable solvent and details about the entire functional groups can be obtained, which is independent of the volatility of the components in the bio-oils; and (2) the

chemical shift intervals for functional groups have been well investigated, and quantitative analysis of fuel (Hao et al., 2016).

3.5. Fuel Oil Properties

The fuel characteristics of the pyrolysis oil obtained under the maximum oil yield circumstances were tested using the ASTM standard technique for petroleum products. Density, API Gravity, Kinematic viscosity, fire point, flash point, HHV and other characteristics were measured, as given in Table 6. Bio-oil contains a variety of unique properties that must be taken into account in each application, including manufacturing, storage, transportation, upgrading, and utilization (Demiral and Ayan, 2011). From Fig.6(b) it is identified that the bio-oil is a dark brown liquid with a Smokey odour. Bio-oil has a density of 850-920 kg/m^3 at 26°C, which is comparable to other bio-oils and denser than biodiesel and petroleum diesel. Bio-oil has a higher density owing to its increased residue concentration. Bio-oil developed from co-pyrolysis of PP, GS and PCW biomass mixture has maximum HHV of 29.1MJ/kg and GS biomass has minimum HHV of 24.3MJ/kg compared with other biomasses. Organic acids, primarily acetic and formic acid, are abundant in bio-oils, resulting in a pH of 4-5 (Varma and Mondal, 2017). As a result, typical construction materials like carbon steel and aluminium are corroded by oils. Corrosiveness is increasingly severe at high temperatures and as the water content rises. Stainless steel is not corroded by the oils (Demiral and Ayan, 2011). The relative density was determined to be under the range of biodiesel fuel reported results. The denser the fuel, the heavier it is and the more difficult it is to burn. The API gravity of medium oil is between 22.3 and 31.1° (i.e., 870 to 920 kg/m^3). The viscosity of liquid fuel is essential to the design and performance of a fuel injection system. The viscosity of a fluid is a measure of its resistance to gravity flow. It will have a significant impact on the fuel injection system's design and operation, as well as the atomization quality and consequent ignition attributes of the fuel. At 50°C, the bio-oil has a kinetic viscosity of 6-10 cSt, which is higher than standard diesel fuel (1.9-4 cSt). Due to its considerable density and viscosity, bio-oil may have difficulty pumping and atomizing in engines, as well as influencing the performance of bio-oil combustion (Varma and Mondal, 2017). As a result, similar to diesel and heavy fuel oil, further upgrading and refining are required to achieve the requisite quality. The flashpoint of liquid fuel is a measurement of its volatility and ignition edge. The higher the flashpoint, the safer it is to handle and the lesser the possibility of an accident caused by vapour ignition. The flashpoint is the liquid temperature at which vapours above a pool of fuel will ignite when a flame is passed across

particles. Bio-oil has a flash and fire point of 85-90℃ and 90-100℃, accordingly, which is equivalent to other bio-oils (Varma et al., 2019).

4. Challenges and Future perspectives

Conversion methodologies of waste to energy process by the pyrolysis process are still relatively novel concept. Therefore, further research works are required to implement a large-scale production and commercialization actions of energy conversion from waste sources through pyrolysis process. Additionally, the novel concept of waste pyrolysis, the cost margin for the collection and processing of waste sources will remain high. Moreover, the reactor construction, maintenance operations and accessing the technical sources are still excessive for biofuel development in most of the countries. Biofuel development from the microwave preheated pyrolysis process has received huge attention for the large-scale conversion due to the exclusive feature of microwave treatment for achieving rapid heating and energy efficient. To achieve the productive commercialization, various novel developments should be experimented to overcome high energy requirement, selection of suitable material for designing the microwave reactor and design of an effective equipment for the condensation process. Furthermore, the continuous microwave assisted pyrolytic reactor will be the major research region, due to the possibility of favourable waste valorisation system with continuous biomass supply. Moreover, the operating conditions and pyrolysis reactor design for the continuous mode still need more research compared to batch mode due to the inadequate knowledge on the biomass supply and instantaneous removal techniques of pyrolysis products. When compared to batch mode, the innovation of microwave assisted pyrolysis of waste biomass by continuous mode will provide better production rate with minimized energy consumption. Therefore, a pyrolytic reactor for continuous mode operation must be developed and experimented with microwave preheating of waste biomasses to overcome the limitations of batch mode operation.

5. Conclusion

In this present study, various biomasses (PP, GS and PCW) were subjected to pyrolysis, co-pyrolysis and catalytic co-pyrolysis processes under the same operating conditions. Among all biomasses used, PP biomass produced a higher bio-oil yield rate of 36.6% during the individual pyrolysis process at 550℃ under 0.25mm particle size. The CaO catalyst aided of three biomass mixtures under microwave pretreatment produced a superior pyrolysis yield of

51.6% due to the cohesive formation of biomass particles. The resultant volatile pyrolysis oil has higher concentrations of hydroxyl group and ethers which are favourable for automotive applications.

Appendix

E-supplementary data for this work can be found in e-version of this paper online.

Credit Author Statement

P Jennita Jacqueline; Investigation, original draft preparation

V ShenbagaMuthuraman; Experimental work

C Karthick; Data validation

Abed Alaswad; Reviewing and Editing

K NanthaGopal; Methodology, Reviewing and editing work

Velvizhi G; Methodology, Reviewing and editing work

Conflict of Interest

There is no conflict of interest in this project.

Acknowledgement

The authors gratefully acknowledge the financial support offered by the Department of Science and Technology-Science and Engineering Research Board, New Delhi, India under the DST-SERB(EEQ) scheme [Project No: EEQ/2018/000725] and Department of Biotechnology, Government of India [Project No. BT/PR31259/PBD/26/756/2019) for providing financial support to carry put this project.

Reference

[1]. Arenas, C.N., Navarro, M.V., Martínez, J.D., 2019. Pyrolysis kinetics of biomass wastes using isoconversional methods and the distributed activation energy model. Bioresour. Technol. 288. https://doi.org/10.1016/j.biortech.2019.121485

[2]. Berrueco, C., Esperanza, E., Mastral, F.J., Ceamanos, J., García-Bacaicoa, P., 2005. Pyrolysis of waste tyres in an atmospheric static-bed batch reactor: Analysis of the gases obtained. J. Anal. Appl. Pyrolysis 74, 245–253. https://doi.org/10.1016/j.jaap.2004.10.007

[3]. Bhattacharjee, N., Biswas, A.B., 2019. Pyrolysis of orange bagasse: Comparative study and parametric influence on the product yield and their characterization. J. Environ. Chem. Eng. 7, 102903. https://doi.org/10.1016/j.jece.2019.102903

[4]. Ceylan, S., Goldfarb, J.L., 2015. Green tide to green fuels: TG-FTIR analysis and kinetic study of Ulva prolifera pyrolysis. Energy Convers. Manag. 101, 263–270. https://doi.org/10.1016/j.enconman.2015.05.029

[5]. Chakraborty, S., Dunford, N.T., Goad, C., 2021. A kinetic study of microalgae, municipal sludge and cedar wood co-pyrolysis. Renew. Energy 165, 514–524. https://doi.org/10.1016/j.renene.2020.11.012

[6]. Demiral, I., Ayan, E.A., 2011. Pyrolysis of grape bagasse: Effect of pyrolysis conditions on the product yields and characterization of the liquid product. Bioresour. Technol. 102, 3946–3951. https://doi.org/10.1016/j.biortech.2010.11.077

[7]. Demirbaş, A., Arin, G., 2002. An overview of biomass pyrolysis. Energy Sources 24, 471–482. https://doi.org/10.1080/00908310252889979

[8]. Fekhar, B., Zsinka, V., Miskolczi, N., 2020. Thermo-catalytic co-pyrolysis of waste plastic and paper in batch and tubular reactors for in-situ product improvement. J. Environ. Manage. 269, 110741. https://doi.org/10.1016/j.jenvman.2020.110741

[9]. Ferreiro, A.I., Giudicianni, P., Grottola, C.M., Rabaçal, M., Costa, M., Ragucci, R., 2017. Unresolved Issues on the Kinetic Modeling of Pyrolysis of Woody and Nonwoody Biomass Fuels. Energy and Fuels 31, 4035–4044. https://doi.org/10.1021/acs.energyfuels.6b03445

[10]. Hao, J., Qi, B., Li, D., Zeng, F., 2021. Catalytic co-pyrolysis of rice straw and ulva prolifera macroalgae: Effects of process parameter on bio-oil up-gradation. Renew. Energy 164, 460–471. https://doi.org/10.1016/j.renene.2020.09.056

[11]. Hao, N., Ben, H., Yoo, C.G., Adhikari, S., Ragauskas, A.J., 2016. Review of NMR Characterization of Pyrolysis Oils. Energy and Fuels 30, 6863–6880. https://doi.org/10.1021/acs.energyfuels.6b01002

[12]. Hu, Y., Wang, H., Lakshmikandan, M., Wang, S., Wang, Q., He, Z., Abomohra, A.E.F., 2021. Catalytic co-pyrolysis of seaweeds and cellulose using mixed ZSM-5 and MCM-41 for enhanced crude bio-oil production. J. Therm. Anal. Calorim. 143, 827–842. https://doi.org/10.1007/s10973-020-09291-w

[13]. Kainthola, J., Shariq, M., Kalamdhad, A.S., Goud, V. V., 2019. Enhanced methane potential of rice straw with microwave assisted pretreatment and its kinetic analysis. J. Environ. Manage. 232, 188–196. https://doi.org/10.1016/j.jenvman.2018.11.052

[14]. Lazzari, E., Schena, T., Marcelo, M.C.A., Primaz, C.T., Silva, A.N., Ferrão, M.F., Bjerk, T., Caramão, E.B., 2018. Classification of biomass through their pyrolytic bio-oil composition using FTIR and PCA analysis. Ind. Crops Prod. 111, 856–864. https://doi.org/10.1016/j.indcrop.2017.11.005

[15]. Liang, J., Yu, Z., Chen, L., Fang, S., Ma, X., 2019. Microwave pretreatment power and duration time effects on the catalytic pyrolysis behaviors and kinetics of water hyacinth. Bioresour. Technol. 286, 121369. https://doi.org/10.1016/j.biortech.2019.121369

[16]. Lin, X., Zhang, Zhifeng, Zhang, Zhijun, Sun, J., Wang, Q., Pittman, C.U., 2018. Catalytic fast pyrolysis of a wood-plastic composite with metal oxides as catalysts. Waste Manag. 79, 38–47. https://doi.org/10.1016/j.wasman.2018.07.021

[17]. Liu, Y., He, Z., Shankle, M., Tewolde, H., 2016. Compositional features of cotton plant biomass fractions characterized by attenuated total reflection Fourier transform infrared spectroscopy. Ind. Crops Prod. 79, 283–286. https://doi.org/10.1016/j.indcrop.2015.11.022

[18]. Lu, Q., Zhang, Z.F., Dong, C.Q., Zhu, X.F., 2010. Catalytic upgrading of biomass fast pyrolysis vapors with nano metal oxides: An analytical Py-GC/MS study. Energies 3, 1805–1820. https://doi.org/10.3390/en3111805

[19]. Matrapazi, V.K., Zabaniotou, A., 2020. Experimental and feasibility study of spent coffee grounds upscaling via pyrolysis towards proposing an eco-social innovation circular economy solution. Sci. Total Environ. 718. https://doi.org/10.1016/j.scitotenv.2020.137316

[20]. McIntosh, S., Nabi, M.N., Moghaddam, L., Brooks, P., Ghandehari, P.S., Erler, D., 2021. Combined pyrolysis and sulphided NiMo/Al2O3 catalysed hydroprocessing in a multistage strategy for the production of biofuels from milk processing waste. Fuel 295, 120602. https://doi.org/10.1016/j.fuel.2021.120602

[21]. Mishra, R.K., Mohanty, K., 2020. Kinetic analysis and pyrolysis behaviour of waste biomass towards its bioenergy potential. Bioresour. Technol. 311, 123480. https://doi.org/10.1016/j.biortech.2020.123480

[22]. Mishra, R.K., Sahoo, A., Mohanty, K., 2019. Pyrolysis kinetics and synergistic effect in co-pyrolysis of Samanea saman seeds and polyethylene terephthalate using thermogravimetric analyser. Bioresour. Technol. 289, 121608. https://doi.org/10.1016/j.biortech.2019.121608

[23]. Mong, G.R., Chong, C.T., Ng, J., Woei, W., Chong, F., Shiung, S., Chyuan, H., Nasir, F., 2020. Microwave pyrolysis for valorisation of horse manure biowaste. Energy Convers. Manag. 220, 113074. https://doi.org/10.1016/j.enconman.2020.113074

[24]. Neves, D., Thunman, H., Matos, A., Tarelho, L., Gómez-Barea, A., 2011. Characterization and prediction of biomass pyrolysis products. Prog. Energy Combust. Sci. 37, 611–630. https://doi.org/10.1016/j.pecs.2011.01.001

[25]. Park, H.J., Heo, H.S., Yoo, K.S., Yim, J.H., Sohn, J.M., Jeong, K.E., Jeon, J.K., Park, Y.K., 2011. Thermal degradation of plywood with block polypropylene in TG and batch reactor system. J. Ind. Eng. Chem. 17, 549–553. https://doi.org/10.1016/j.jiec.2010.11.002

[26]. Pimenidou, P., Dupont, V., 2012. Characterisation of palm empty fruit bunch (PEFB) and pinewood bio-oils and kinetics of their thermal degradation. Bioresour. Technol. 109, 198–205. https://doi.org/10.1016/j.biortech.2012.01.020

[27]. Ren, X., Feng, X., Cao, J., Tang, W., Wang, Z., Zhao, J., Zhang, L., Wang, Y., Zhao, X., 2020. Working Title : Catalytic conversion of coal and biomass volatiles : A review Catalytic Conversion of Coal and Biomass Volatiles : A Review. https://doi.org/10.1021/acs.energyfuels.0c01432

[28]. Rout, T., Pradhan, D., Singh, R.K., Kumari, N., 2016. Journal of Environmental Chemical Engineering Exhaustive study of products obtained from coconut shell pyrolysis. Biochem. Pharmacol. https://doi.org/10.1016/j.jece.2016.02.024

[29]. Sakulkit, P., Palamanit, A., Dejchanchaiwong, R., Reubroycharoen, P., 2020. Characteristics of pyrolysis products from pyrolysis and co-pyrolysis of rubber wood and oil palm trunk biomass for biofuel and value-added applications. J. Environ. Chem. Eng. 8. https://doi.org/10.1016/j.jece.2020.104561

[30]. Karthick C., Nanthagopal K., 2021. A comprehensive review on ecological approaches of waste to wealth strategies for production of sustainable biobutanol and its suitability in automotive applications. Energy Conversion and Management. 239, 114219. https://doi.org/10.1016/j.enconman.2021.114219

[31]. Singh, R.K., Patil, T., Sawarkar, A.N., 2020. Pyrolysis of garlic husk biomass: Physico-chemical characterization, thermodynamic and kinetic analyses. Bioresour. Technol. Reports

12. https://doi.org/10.1016/j.biteb.2020.100558

[32]. Smets, K., Adriaensens, P., Vandewijngaarden, J., Stals, M., Cornelissen, T., Schreurs, S., Carleer, R., Yperman, J., 2011. Water content of pyrolysis oil: Comparison between Karl Fischer titration, GC/MS-corrected azeotropic distillation and 1H NMR spectroscopy. J. Anal. Appl. Pyrolysis 90, 100–105. https://doi.org/10.1016/j.jaap.2010.10.010

[33]. Soni, B., Karmee, S.K., 2020. Towards a continuous pilot scale pyrolysis based biorefinery for production of biooil and biochar from sawdust. Fuel 271. https://doi.org/10.1016/j.fuel.2020.117570

[34]. Struhs, E., Hansen, S., Mirkouei, A., Ramirez-Corredores, M.M., Sharma, K., Spiers, R., Kalivas, J.H., 2021. Ultrasonic-assisted catalytic transfer hydrogenation for upgrading pyrolysis-oil. Ultrason. Sonochem. 73, 105502. https://doi.org/10.1016/j.ultsonch.2021.105502

[35]. Suriapparao, D. V., Vinu, R., Shukla, A., Haldar, S., 2020. Effective deoxygenation for the production of liquid biofuels via microwave assisted co-pyrolysis of agro residues and waste plastics combined with catalytic upgradation. Bioresour. Technol. 302. https://doi.org/10.1016/j.biortech.2020.122775

[36]. Varma, A.K., Mondal, P., 2017. Pyrolysis of sugarcane bagasse in semi batch reactor: Effects of process parameters on product yields and characterization of products. Ind. Crops Prod. 95, 704–717. https://doi.org/10.1016/j.indcrop.2016.11.039

[37]. Varma, A.K., Thakur, L.S., Shankar, R., Mondal, P., 2019. Pyrolysis of wood sawdust: Effects of process parameters on products yield and characterization of products. Waste Manag. 89, 224–235. https://doi.org/10.1016/j.wasman.2019.04.016

[38]. Veses, A., Aznar, M., Martínez, I., Martínez, J.D., López, J.M., Navarro, M. V., Callén, M.S., Murillo, R., García, T., 2014. Catalytic pyrolysis of wood biomass in an auger reactor using calcium-based catalysts. Bioresour. Technol. 162, 250–258. https://doi.org/10.1016/j.biortech.2014.03.146

[39]. Volpe, R., Zabaniotou, A., Skoulou, V.K., 2018. Synergistic effects of lignin and cellulose during pyrolysis of agricultural waste . Synergistic effects of lignin and cellulose during pyrolysis of. https://doi.org/10.1021/acs.energyfuels.8b00767

[40]. Vuppaladadiyam AK., Antunes E., Vuppaladadiyam VS., Shehzad F., Somasundaram M., Memon MZ., Song Q., Dong W., Duan H., 2021. Discernment of synergy during the co-pyrolysis of lipid-extracted microalgae and digested municipal solid waste: a thermogravimetric–mass spectrometric study. Journal of Chemical Technology &

Biotechnology. https://doi.org/10.1002/jctb.6702

[41]. Wang, D., Xiao, R., Zhang, H., He, G., 2010. Comparison of catalytic pyrolysis of biomass with MCM-41 and CaO catalysts by using TGA-FTIR analysis. J. Anal. Appl. Pyrolysis 89, 171–177. https://doi.org/10.1016/j.jaap.2010.07.008

[42]. Wu, Q., Wang, Y., Jiang, L., Yang, Q., Ke, L., Peng, Y., Yang, S., Dai, L., Liu, Y., Ruan, R., 2020. Microwave-assisted catalytic upgrading of co-pyrolysis vapor using HZSM-5 and MCM-41 for bio-oil production: Co-feeding of soapstock and straw in a downdraft reactor. Bioresour. Technol. 299. https://doi.org/10.1016/j.biortech.2019.122611

[43]. Xiao, R., Yang, W., Cong, X., Dong, K., Xu, J., Wang, D., Yang, X., 2020. Thermogravimetric analysis and reaction kinetics of lignocellulosic biomass pyrolysis. Energy 201, 117537. https://doi.org/10.1016/j.energy.2020.117537

[44]. Yang, H., Yan, R., Chen, H., Lee, D.H., Zheng, C., 2007. Characteristics of hemicellulose, cellulose and lignin pyrolysis. Fuel 86, 1781–1788. https://doi.org/10.1016/j.fuel.2006.12.013

[45]. Zhang, L., Yang, Z., Li, S., Wang, X., Lin, R., 2020. Comparative study on the two-step pyrolysis of different lignocellulosic biomass: Effects of components. J. Anal. Appl. Pyrolysis 152. https://doi.org/10.1016/j.jaap.2020.104966

[46]. Zhang, X., Yu, Z., Lu, X., Ma, X., 2021. Catalytic co-pyrolysis of microwave pretreated chili straw and polypropylene to produce hydrocarbons-rich bio-oil. Bioresour. Technol. 319. https://doi.org/10.1016/j.biortech.2020.124191

[47]. Zhao, J., Cao, J., Wei, F., Feng, X., Yao, N., Zhao, Y., Al, E., 2020. Catalytic reforming of lignite pyrolysis volatiles over sulfated HZSM-5 : Significance of the introduced extra-framework Al species. Fuel 273, 117789. https://doi.org/10.1016/j.fuel.2020.117789

[48]. Zhen Z., Wang H., Yue Y., Li D., Song X., Li J., 2020. Determination of water content of crude oil by azeotropic distillation Karl Fischer coulometric titration. Analytical and Bioanalytical Chemistry. 412, 4639-45. https://doi.org/10.1007%2Fs00216-020-02714-5

Credit Author Statement

P Jennita Jacqueline; Investigation, original draft preparation

V ShenbagaMuthuraman; Experimental work

C Karthick; Data validation

Abed Alaswad; Reviewing and Editing

K Nanthagopal; Methodology, Reviewing and editing work

Velvizhi G; Methodology, Reviewing and editing work

Declaration of interests

The authors declare that they have no known competing financial interests or personal relationships that could have appeared to influence the work reported in this paper.

Highlights

- Catalytic and non-catalytic co-pyrolysis processes are used for bio-oil production
- Microwave preheated co-pyrolysis yielded higher bio-oil at 0.25 mm particle size
- CaO aided co-pyrolysis of PP, GS and PCW showed bio-oil yield of 51.6%
- FE-SEM results confirmed the changes in morphological structure of biomasses with CaO
- NMR results of pyrolysis oil exposed the presence the hydroxyl radicals and ethers

List of Figures

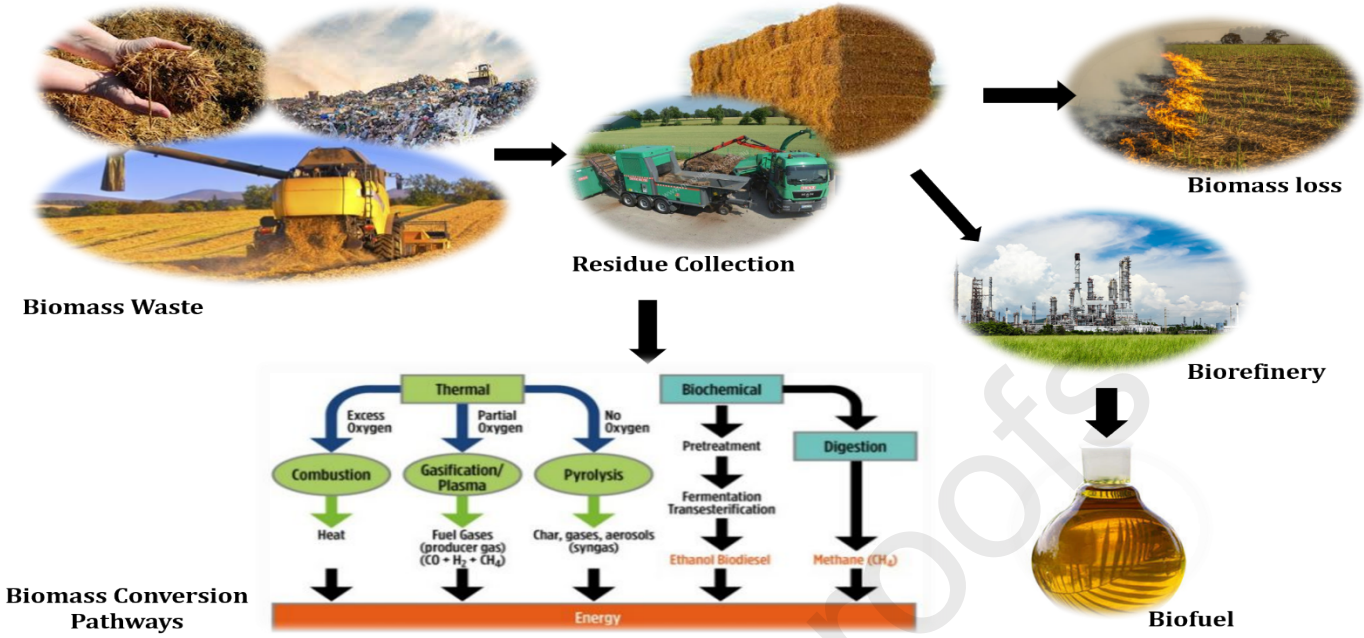

Fig.1: Waste Management Strategy for biofuel production

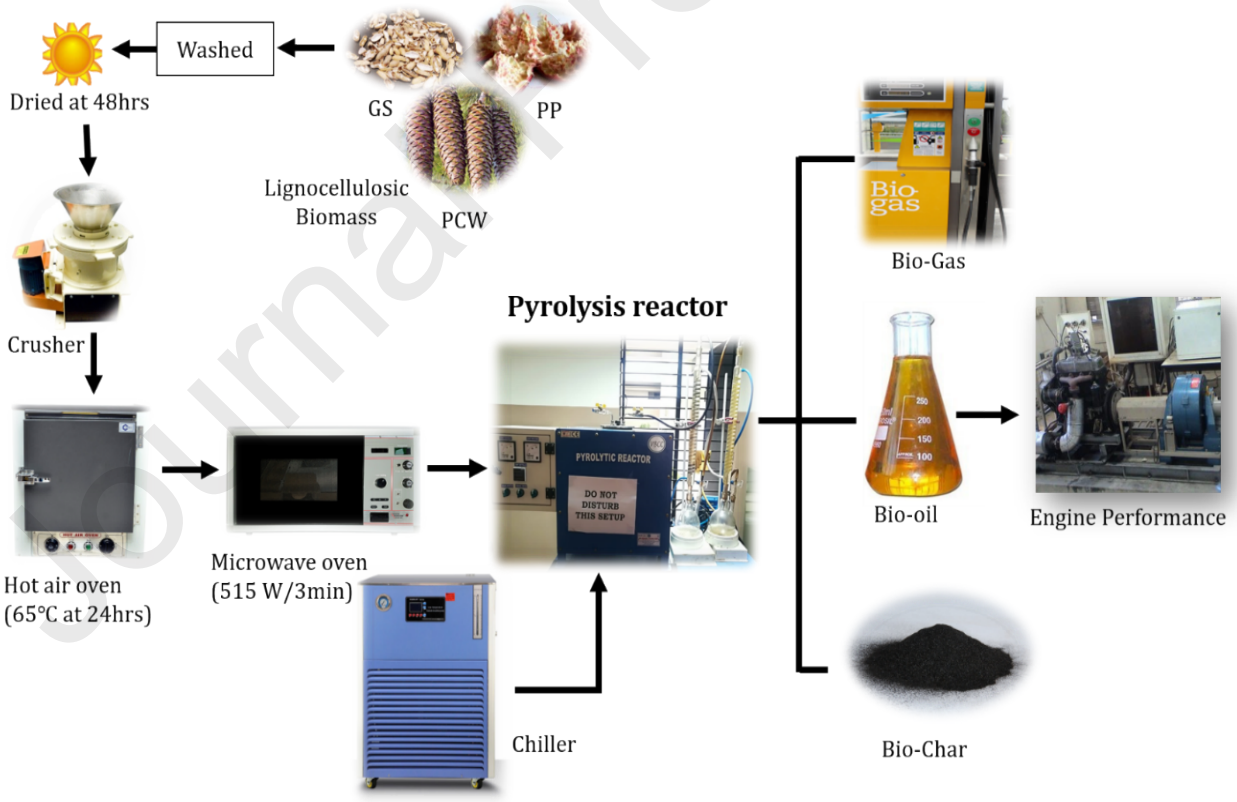

Fig.2: Schematic representation of the pyrolysis process

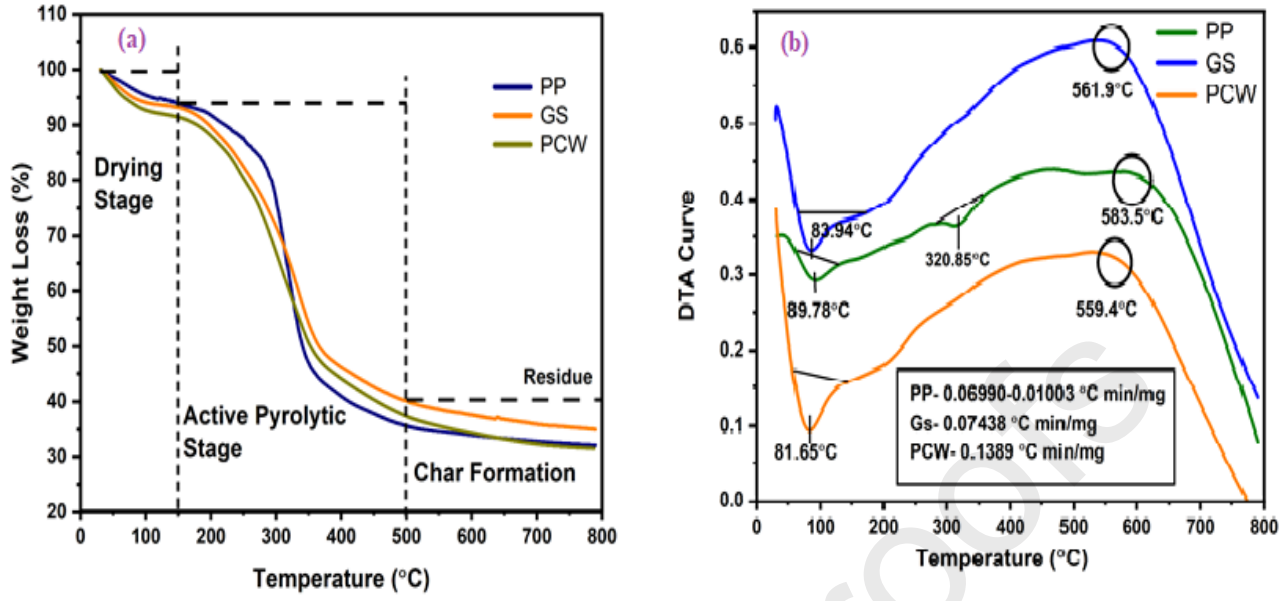

Fig.3: Analysis Curves of different biomasses (a) TGA (b) DTA

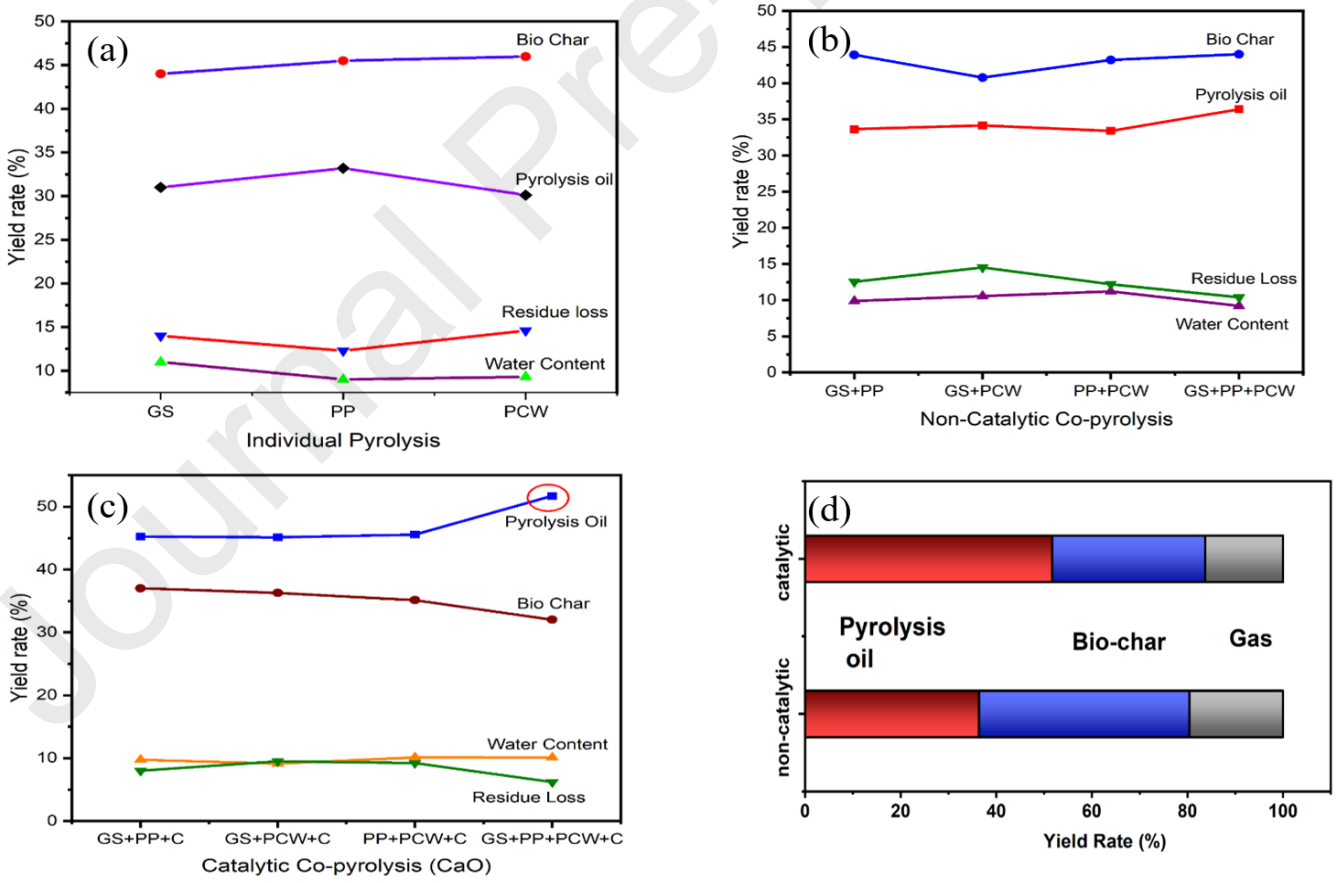

Fig.4: Different stages of pyrolysis product yield rate (a) individual (b) Non-catalytic co-pyrolysis (c) Catalytic co-pyrolysis (d) Optimized yield rate

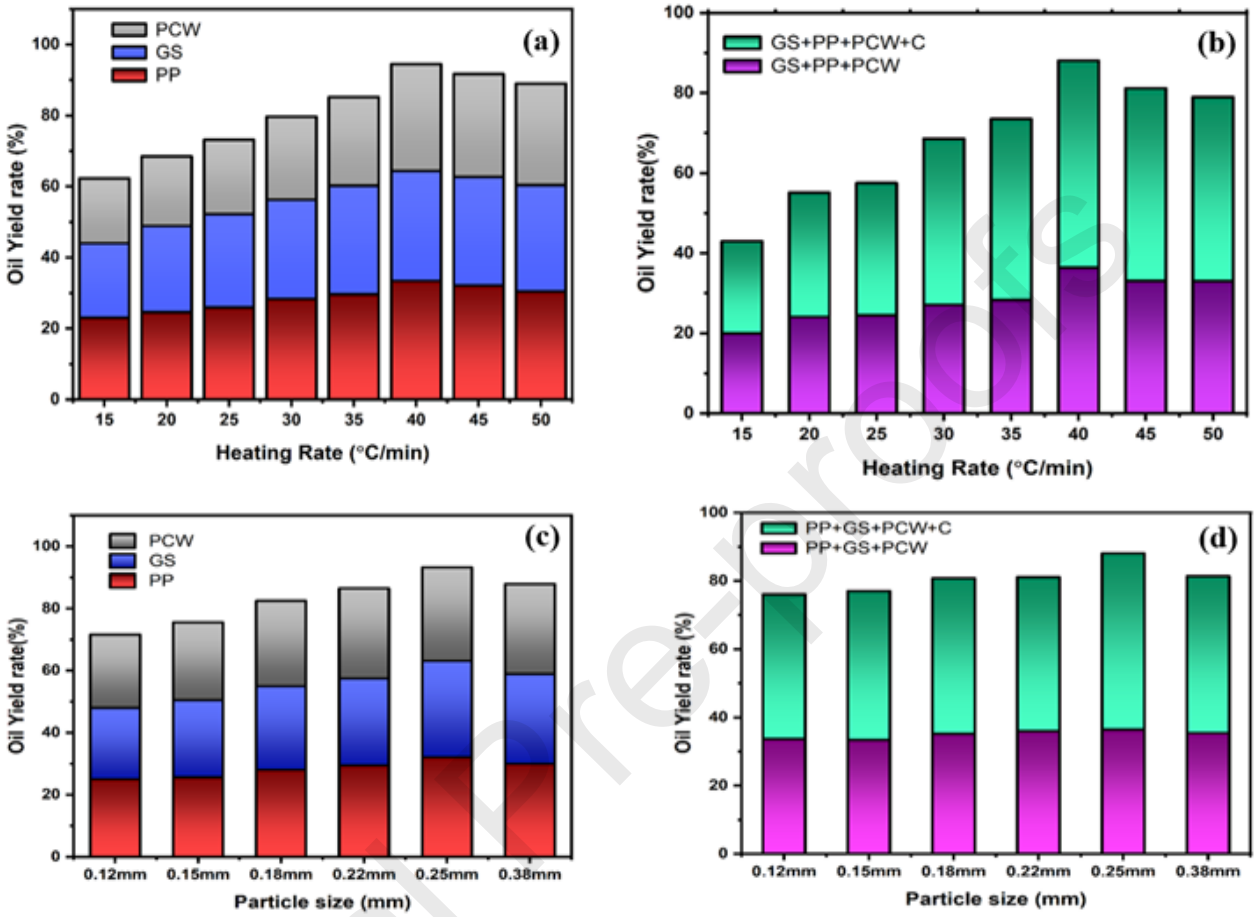

Fig.5 (a) Influence of heating rates on individual three pyrolysis bio-oil yield, (b)Influence of heating rates on Bio-oil yield of non-catalytic and catalytic co-pyrolysis, (c) Influence of particle size on individual three pyrolysis bio-oil yield, (d) Influence of particle size on Bio-oil yield of non-catalytic and catalytic co-pyrolysis

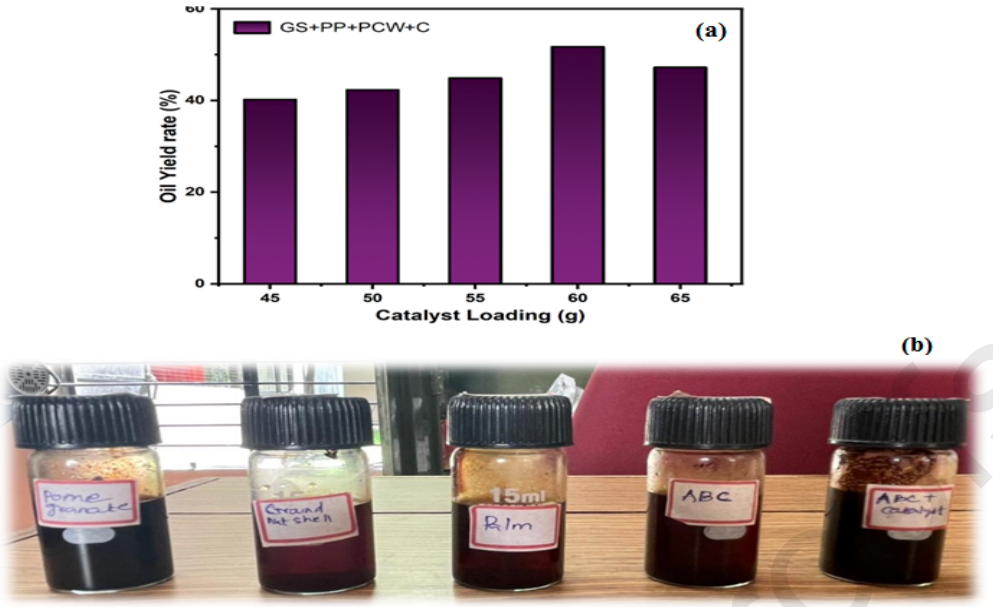

Fig.6 (a) Influence of different rates of catalyst on bio-oil yield of catalytic co-pyrolysis, (b) Outcome of pyrolysis oil in different experiments.

List of Tables

Table 1: Instrument used in characterization analysis of biomasses and product yield.

sis	Characterization	Instruments	Specification
S	Biomasses and biochar	Perkin Elmer-2400	Ultimate/ Elemental analys
DTA	Biomasses	TA Instruments, USA. Model: SDT Q600	Thermal stability and Temperature
	Experiment biomass samples and biochar	MODEL: Thermo Nicolet iS50 with inbuilt ATR made by Thermo Fisher Scientific	Functional group and chemical clas
d EDS	Biomasses	Thermo Fisher FEI Quanta 250 FEG	Morphological Structure and composit
iscosity	Pyrolysis oil	Redwood viscometer	Oil thickness and viscosity
ng value	Pyrolysis oil	Digital Bomb calorimeter	Oil energy density
re point	Pyrolysis oil	Pensky marten	Ignition properties
IR	Pyrolysis oil	400 MHz (Bruker)	Spectrum and Hydrogen type

Table 2: Operational Conditions for different Pre-heating Experiments

Experimental Code	Biomass Sample	Proportional PP (%)	Proportional PCW (%)	Proportional GS (%)	Micro oven Condition(W/min)	Micro Oven time(min)	Pyrolysi Oil Yiel (%)
PE1					887.16	2	Average

PE1.1	PP	100	0	0	818.91	3	Higher
PE1.2					545.94	3	Higher
PE2	GS	0	100	0	887.16	2	Lesser
PE2.1					818.91	3	Lesser
PE2.2					545.94	3	Average
PE3	PCW	0	0	100	887.16	2	Lesser
PE3.1					818.91	3	Average
PE3.2					545.94	3	Average
PE4	PP+PCW	50	50	0	818.91	3	Average
PE4.1					545.94	3	Higher
PE5	PP+GS	50	0	50	818.91	3	Higher
PE5.1					545.94	3	Higher
PE6	PCW+GS	0	50	50	818.91	3	Average
PE6.1					545.94	3	Average
PE7	PP+GS+PCW	50	50	50	545.94	3	Higher

Table 3: Various Proportional Catalyst CaO in different Pre-heating experimental conditions

Experimental Code	**Biomasses Proportional (PP+GS+PCW) (%)**	**Catalyst (CaO) Proportional (%)**	**Micro oven Condition (W/min)**	**Micro Oven time (min)**	**Pyrolysis Oil Yield (%)**
CPE1	80	20	545.94	3	Higher
CPE1.1			818.91	2	Average
CPE2	70	30	545.94	3	Higher
CPE2.1			818.91	2	Lesser
CPE3	60	40	545.94	3	Higher
CPE3.1			818.91	2	Average
CPE4	50	50	545.94	3	Average
CPE4.1			818.91	2	Average
CPE5	40	60	545.94	3	Average
CPE5.1			818.91	2	Lesser

Table 4: Ultimate analysis of biomass raw and biochar

	C (wt.%)	**H (wt.%)**	**O (wt.%) [a]**	**N (wt.%)**	**S (wt.%)**	**H/C ratio**	**O/C ratio**	**Empirical Formula**
(PP)	50.02	6.60	43.28	0.08	0.02	1.57	0.65	$CH_{1.57}O_{0.65}N_{0.00}$

GS)	45.08	5.39	49.03	0.501	-0.01	1.42	0.81	$CH_{1.42}O_{0.81}N_{0.00}$
(PCW)	44.06	4.92	50.15	0.08	-0.01	1.33	0.85	$CH_{1.33}O_{0.85}N_{0.01}$
	80.58	3.51	15.4	0.50	0.01	0.51	0.14	$CH_{0.51}O_{0.14}N_{0.00}$
	78.08	4.52	17.04	0.35	0.01	0.69	0.16	$CH_{0.69}O_{0.16}N_{0.00}$
	76.72	5.52	17.73	0.18	0.01	0.85	0.17	$CH_{0.85}O_{0.17}N_{0.00}$

[a.]By difference, [b.]Calculated by Dulong equation (33.5 × C + 142.3 × H - 14.5 × N- 15.4 ×O (MJ/Kg)).

Table 5: ^{1}H NMR characterization of bio-oils.

Assignments	**Chemical Shift- Peak**			
	PP	**GS**	**PCW**	**PP+GS+PCW**
C=C	5.92	-	5.23	6.5
-CH_n-O-	5.7	4.14	4.5	5.24
Ar- CH_2-O-	4.47	-	4.05	4.25
Ether, methoxyl	3.79	3.71	3.61	3.77
Alcohols, methylene-di benzene	3.568	3.26	3.65	3.27
CH_3C=O, CH_3-Ar	3.36	-	3.27	2.086
CH_2C=O, aliphatics	2.08	2.04	2.04	2.041
Aliphatics α to heteroatom or unsaturation	1.91	1.913	1.92	1.92
-CH_2, aliphatic OH	1.12	-	-	-
-CH_3, -CH_2	1.09	1.13	1.05	-
β-CH_3, CHγ	1.01	1.02	1.00	1.02

Table 6: Physical properties of pyrolysis bio-oil:

Properties	**PP**	**GS**	**PCW**	**PP+GS+PCW**	**PP+GS+PCW+ CaO**
pH	4.84	4.68	4.53	4.46	4.67
Kinematic Viscosity at 50°C (Centistokes)	7.8	6.1	7.1	8.56	9.56
Density at 26°C (Kg/m^3)	906	912	890	840	860

Higher Heating Value (MJ/kg)	27.5	24.3	25.6	29.1	27.4
API Gravity	24.68	23.65	27.48	36.95	33.03
Flash Point (°C)	89	87	87	88	89
Fire Point (°C)	95	97	89	91	96